Science of the Total Environment 903 (2023) 166421

Contents lists available at ScienceDirect

Science of the Total Environment

journal homepage: www.elsevier.com/locate/scitotenv

Tetrabromobisphenol a and its alternative tetrachlorobisphenol a induce oxidative stress, lipometabolism disturbance, and autophagy in the liver of male *Pelophylax nigromaculatus*

Yu Han [a], Hongmei Yang [a], Zhiqun Liu [a], Chao Hu [a], Imane Lamine [b], Zhiquan Liu [a], Panpan Gao [a], Yanming Sui [c], Pei Zheng [d], Hangjun Zhang [a], Xiuying Jia [a,e,*]

[a] Hangzhou Normal University, Hangzhou, 311121, China
[b] Laboratory of Aquatic Systems, Marine and Continental Ecosystems, Department of Biology, Faculty of Sciences, Ibn Zohr University, Agadir 80000, Morocco
[c] School of Marine and Biological Engineering, Yancheng Institute of Technology, Yancheng, 224002, China
[d] Dianshan branch of Ecological Environment Bureau, Zhoushan, 316299, China
[e] Hangzhou City University, Hangzhou, 310015, China

HIGHLIGHTS

- TBBPA and TCBPA induced liver toxicity in black spotted frog.
- TBBPA and TCBPA trigger oxidative damage and autophagy in black spotted frog.
- TBBPA and TCBPA could bind with PPARγ amino acid residues.
- Lipid accumulation is significantly aggravated by TBBPA and TCBPA exposure.

GRAPHICAL ABSTRACT

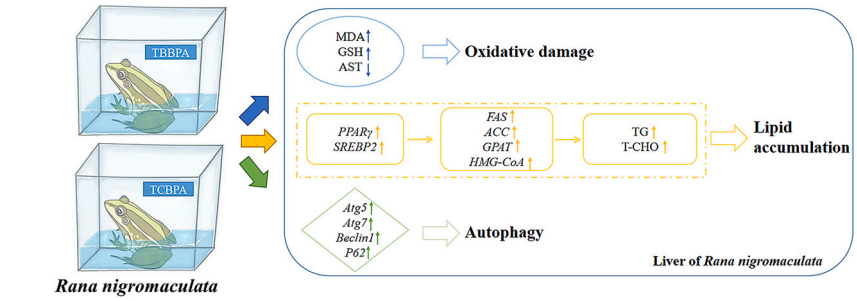

Rana nigromaculata
Hepatotoxicity : TCBPA ≥ TBBPA

ARTICLE INFO

Editor: Damià Barceló

Keywords:
P. nigromaculatus
TBBPA
TCBPA
Lipid metabolism
Autophagy
Oxidative stress

ABSTRACT

Tetrabromobisphenol A (TBBPA) and tetrachlorobisphenol A (TCBPA) have been widely used as flame retardants. However, their potential health risks to organisms have raised concerns, particularly for liver toxicity. Present study aimed to explore the toxic effects of TCBPA and TBBPA on black-spotted frogs (*Pelophylax nigromaculatus*) liver oxidative stress, autophagy, and lipid accumulation. After exposure to 0.001, 0.01, 0.1, and 1 mg/L TBBPA and TCBPA for 14 days, the content of cholesterol and triglyceride were significantly elevated. In addition, the malondialdehyde level rose greatly in dose dependent. However, the glutathione level declined in high TBBPA groups (0.01 and 0.1 mg/L). Furthermore, expressions of *Beclin1*, *Atg5*, and *Atg7* were significantly increased, while *p62 was* markedly declined, respectively. Results obstained suggested that TBBPA and TCBPA exposure induced liver toxicity in black-spotted frog. This study provided insights into the toxicity mechanism of bisphenol flame retardants in amphibians and will aid in the ecological risk assessment of flame retardants.

* Corresponding author at: Hangzhou Normal University, Hangzhou, 311121, China.
E-mail address: jiaxiuying0523@163.com (X. Jia).

https://doi.org/10.1016/j.scitotenv.2023.166421
Received 3 June 2023; Received in revised form 30 July 2023; Accepted 17 August 2023
Available online 23 August 2023

1. Introduction

Tetrabromobisphenol A (TBBPA) and tetrachlorobisphenol A (TCBPA) are widely used as flame retardants in a variety of consumer products, including electrical gadgets, fabrics, and polymers used in the electronics sector (Bjermo et al., 2017; Jarosiewicz et al., 2017). With annual output exceeding 2 million tons, TBBPA is account for approximately 60 % of the global BFR (Brominated flame retardants) market (Jarosiewicz et al., 2017; Law et al., 2006; Yu et al., 2019). However, with its volatilization, leaching, and abrasion, TBBPA inevitably enters the environment (Kim et al., 2016). For example, He et al. (2013) and Yang et al. (2012) found that TBBPA concentrations in Dongjiang River and Chaohu Lake was 2.83 and 4870 ng/L, respectively. What's more, the content of TCBPA was 142.5–542.6 ng/g dry weight in river silt and sediment (Song et al., 2014a,Song et al., 2014b; Yuan et al., 2010). More seriously, it has been detected that the concentration of TBBPA was 42 ng/g and 0.143 ng/mL in human breast milk and pregnant women serum, respectively (Huang et al., 2020; Li et al., 2020).

Studies have shown that BFR have potential hepatotoxicity (Jia et al., 2022; Ma et al., 2015; Yao et al., 2021). For example, TBBPA and TCBPA exposure could induce PPARγ overexpression and metabolic dysfunction of human hepatocellular carcinoma HepG2 cells (Yu et al., 2022). In addition, after incubation with TBBPA and TBBPS for 24 h, single-stranded DNA was broken in human peripheral blood mononuclear cells, which eventually led to DNA damage (Baranska et al., 2022). Moreover, many studies indicated that TBBPA and TCBPA might have adverse effects on the health of aquatic organisms (Zhang et al., 2022; Liu et al., 2023; Gong et al., 2023). For instance, Song et al. (2014a) found that after exposure to TBBPA and TCBPA for 21 days, the development of zebrafish embryos was slowed and the body showed edema and bleeding. After exposure to TBBPA and TCBPA for 14 days, the liver of black-spotted frog (*Pelophylax nigromaculatus*) was damaged through reactive oxygen species-dependent mitochondrial pathway apoptosis (Jia et al., 2022).

As an important energy source for organisms, the homeostasis of lipid metabolism plays an important role in organisms (Lin et al., 2022a). Previus study showed that oxidative stress could restrict mitochondrial function and decrease fatty acid metabolism, which finally lead to lipid accumulation (Pan et al., 2018). Other study also revealed that oxidative stress might trigger lipid accumulation in BRL-3A cells through the Keap1/Nrf2 pathway (Zhao et al., 2018). Meanwhile, Gong et al. (2023) found that TBBPA could cause oxidative stress in carp which finally induce apoptosis and necroptosis. What's more, peroxisome proliferator-activated receptor gamma (PPARγ), Acetyl-CoA carboxylase (ACC) and fatty acid synthase (FAS) played a critical role to regulate lipid synthesis (Choi et al., 2022; Lee et al., 2022; Su et al., 2019; Huo et al., 2022; Luo et al., 2020). At the same time, studies revealed that TBBPA and TCBPA could alter the expression of PPARγ, the activity of ACC and FAS (Riu et al., 2011; Garoche et al., 2021; Kowalczyk et al., 2023). However, the impact of TBBPA and TCBPA on hepatic lipid balance in the liver of *P. nigromaculatus* are not clear yet.

Numerous studies have shown that a deficiency in autophagy decreases the formation of lipid droplets both in vivo and in vitro (Shibata et al., 2009, 2010). As a lipid buffer system, lipid droplets isolate fatty acids produced by autophagous degradation of membrane organelles and reduce lipid toxicity (Nguyen et al., 2017). Moreover, autophagy can be initiated by many stress and toxicological responses as well as pathological reactions (Moore et al., 2008). One study indicated that exposure to BPA and nanoparticles in a mixed toxicology trial caused excessive autophagy and apoptosis in rat testes with higher expression of *Beclin-1* and *Atg5* (Su et al., 2018). Similarly, TBBPA and TCBPA could induce carp neutrophil autophagy after expourse 3 h (Gong et al., 2023). Due to the close relationship between autophagy and lipid homeostasis, the effect of TBBPA and TCBPA on liver autophagy in *P. nigromaculatus* were investigated.

As the typical amphibian in china, the black-spotted frog plays an important role in maintaining the biodiversity and system stability of farmland ecosystems. After the frog was listed as an endangered animal in 2004, its population continued to decline (IUCN, 2023). One known reason for this decline is the occurrence of environmental contaminants (Lent et al., 2021). Amphibians are particularly vulnerable to the adverse effects of environmental pollutants due to their unique living characteristics and a highly permeable skin (Siviter et al., 2021). Therefore, they can serve as a useful indicator of environmental pollution. Previous experiments showed that *P. nigromaculatus* is highly sensitive to environmental contaminant, which might be a suitable organism to assess the degree of environmental contamination (Zhang et al., 2019; Lin et al., 2022a; Lin et al., 2022b; Tang et al., 2018).

Although a few studies have demonstrated the impact of TBBPA and TCBPA on liver toxicity, the precise mechanism remains unclear. Therefore, present study focused on lipid metabolic toxicity, oxidative injury, and autophagy in the liver caused by TBBPA and TCBPA. We hypothesize that oxidative stress and autophagy associated with lipid metabolism may contribute to liver damage produced by TBBPA and TCBPA. The results of this study will not only influence future research but also provide a fresh theoretical framework for understanding the harmful impacts of TBBPA and TCBPA on amphibian populations.

2. Materials and methods

2.1. Chemicals

The TBBPA and TCBPA were acquired from Aladdin Industrial Company (CAS: 79–94-7) and TCI Industrial Development Corporation (CAS: 79–95-8), respectively. Dimethyl sulfoxide (DMSO) was bought from Lingfeng Chemical Reagent Corporation (CAS: 67–68-5). The purity and solubility of TBBPA and TCBPA were listed in Table 1. Nanjing jiancheng Bioengineering Inc. supplied the enzyme-linked immunosorbent assay kits used to measure total cholesterol (T-CHO, A111–1-1), TGs (A110–1-1), glutathione (GSH, A003–1-2), glutamic oxalacetic transaminase (AST, C010–2-1), and malondialdehyde (MDA, A003–1-2). Invitrogen supplied the TRIzol® Plus RNA Purification Kit and SuperScriptTM III First-Strand Synthesis SuperMix for quantitative real-time PCR (CAS: 11752–050).

2.2. Animals and treatment condition

Healthy adult male frogs (*P. nigromaculatus*, weights: 30 ± 5 g) were purchased from Huzhou, Zhejiang, China. After acclimating for 3 days, 200 frogs were randomly assigned to 10 tanks, with each tank (0.3 m × 0.3 m × 0.6 m) containing 2 L freshwater and 20 frogs. The frogs were acclimated in 50 ± 5 % relative humidity, with 12/12 h of light/dark, temperature 20–22 °C, pH 6.4–7.7, and dissolved oxygen exceeding 6.4 mg/L. The TBBPA and TCBPA were dissolved with DMSO at a final concentration of <0.5 %. According to Zhang et al. (2018), the chosen exposure concentrations of TBBPA and TCBPA were 0, 0.001, 0.01, 0.1, and 1 mg/L. The working concentrations of TBBPA and TCBPA were determined and listed in Table 2.

The earthworm (*Eisenia fetida*) was fed to the frogs twice a day (8:00 and 18:00), and the aerated water was replaced using static displacement every day. After 14 days, the frogs were weighed, dissected, and samples taken from them following euthanasia. Within a short amount

Table 1
Information of TBBPA, TCBPA and DMSO.

Chemicals	Molecular formula	CAS number	solubility	purity
TBBPA	$C_{15}H_{12}Br_4O_2$	79–94-7	<1 mg/mL	≥ 98 %
TCBPA	$C_{15}H_{12}Cl_4O_2$	79–95-8	–	≥ 98 %
DMSO	C_2H_6OS	67–68-5	greater than or equal to 100 mg/mL at 68 °F	≥ 99.5 %

Table 2
Measured background and theworking concentrations of TBBPA and TCBPA tested (Mean ± SE) in each experimental group.

TBBPA	Theoretical concentration (mg/L)	0.001	0.01	0.1	1
	Actual concentration (mg/L)	0.0011 ± 0.0001	0.0107 ± 0.0009	0.0995 ± 0.0015	0.9883 ± 0.0125
TCBPA	Theoretical concentration (mg/L)	0.001	0.01	0.1	1
	Actual concentration (mg/L)	0.0010 ± 0.0001	0.0099 ± 0.0008	0.1039 ± 0.0090	0.1039 ± 0.0090

of time, blood was drawn, and the livers of three frogs from each group were extracted, cleaned, and preserved for morphological analysis. Other livers were promptly frozen in liquid nitrogen and kept at −80 °C.

2.3. Oil red O staining

Oil Red O staining was performed according to Zhang et al. (2019). In brief, three frogs livers were fixed with neutral formalin. Frozen liver tissue pieces were fixed in neutral formalin for 15 min before staining with Oil Red O and hematoxylin for 1 min. The stained sections were then refrozen, mounted with glycerogelatin, and examined under a microscope.

2.4. AST in serum measurement

The blood of three frogs was spun at 4000 *g* for 10 min at 4 °C (Eppendorf, 5427R, Germany). Then, the AST activities of frog serum were measured by AST kit following the manufacturer's instructions.

2.5. MDA and GSH content measurements

Liver tissues were homogenized in cold phosphate-buffered saline (PBS, three replicates, pH 7.4) and the residue collected. The MDA and GSH levels were measured using the appropriate kits, following the manufacturer's instructions.

2.6. T-CHO content measurement

The T-CHO (three replicates) content was determined using the COD-PAP method. Cholesterol esters were broken down by cholesterol esterase into cholesterol. Then, cholesterol was broken-down by cholesterol oxidase into cholesterone and hydrogen peroxide. Red quinone molecules were produced by the reaction of hydrogen peroxide with phenol and 4-aminoantipyrine. The optical density of compounds containing quinones was determined at 510 nm using a spectrophotometer.

2.7. TG content measurement

The TG (three replicates) content was determined using the GPO-PAP method. Lipase converts TG into glycerin, which is then broken-down by glycerol kinase to produce glycerol-3-phosphate. Hydrogen peroxide is produced when glycerol triphosphate is oxidized by glycerol 3-phosphate oxidase. Hydrogen peroxide combines with 4-aminoantipyrine and 4-chlorophenol to form red quinone compounds. The TG kit was used to determined TG content and the optical density of the compound was measured using a spectrophotometer at a wavelength of 510 nm.

2.8. The qPCR

Total RNA in the liver was extracted using a TRIzol® Plus RNA Purification Kit (three replicates). The total RNA was isolated, purified by RNase-Free DNase Set, and detected using an ultraviolet spectrophotometer in accordance with the manufacturer's directions. The qPCR was used to finish the reverse-transcription experiment using the Super-ScriptTM III First-Strand Synthesis SuperMix. Primer Premier 6.0 and Beacon Designer 7.8 were used to create the qPCR primers (Table 3). Then, qPCR was carried out using a CFX 384 Touth™ Real-Time PCR Detection System (Bio-Rad, USA). The reaction system contained 1.0 μL of cDNA, 0.5 μL of forward primer (10 μM), 0.5 μL of reverse primer (10 μM), and 10.0 μL of Power SYBR® Green Master Mix (Applied Biosystems, USA). The thermocycler was programmed for 1 min of denaturation at 95 °C, followed by 40 cycles of 15 s at 95 °C and 25 s at 63 °C for annealing and extension. The CT ($2^{-\Delta\Delta Ct}$) method was used to measure the level of gene expression.

2.9. Molecular docking

The structure of PPARγ (template PDB ID, PPARγ: 3e00.1.B) was modeled using the homology modeling service of SWISS-MODEL (https://swissmodel.expasy.org/). The PubChem website provided the chemical formulas for TBBPA and TCBPA (https://pubchem.ncbi.nlm.nih.gov/). Software version 4.2.6 of AutoDock Tools was used to obtain the available ligand and receptor (Scripps Research Institute, USA). AutoDock Vina 1.1.2 was used for the molecular docking, with the minimized shapes serving as input structures. Pictures were prepared using PyMol version 2.6 (Delano Scientific LLC, USA).

2.10. Statistical analysis

The data were analyzed using Graphpad Prism 8.1. One-way analysis of variance was used to determine the differences between the experimental data of the control and exposure groups. Dates were analyzed by Kolmogorov-Smirnoy test and all of them conform to a normal distribution (Table S1). The datas were presented as mean ± standard error of the mean (SEM), with $P < 0.05$ indicating a significant difference, and $P < 0.01$ indicating an extremely significant difference.

3. Results

3.1. TBBPA and TCBPA induce hepatic oxidative stress

We investigated the impact of TBBPA and TCBPA on liver health using the AST activity in serum, as well as MDA and GSH levels in the liver (Fig. 1A-C). Compare with control, the AST activity was rising at the low concentration (0.001 mg/L), and the increase was noticeably higher with TBBPA ($P < 0.01$). The AST activity was significantly higher in the group treated with 0.01 mg/L TCBPA than the 0.01 mg/LTBBPA group ($P < 0.01$, Fig. 1A). Compared to the control, all TBBPA and TCBPA treatment groups showed a marked increase in MDA content in the liver ($P < 0.01$, Fig. 1B). The increase was more prominent in the TCBPA than the TBBPA group, with significant differences for the groups that received 0.1 mg/L ($P < 0.05$). Additionally, compared to the control, both the 0.01 and 0.1 mg/L TBBPA treatment groups showed a decrease in GSH levels after 2 weeks exposure (Fig. 1C).

3.2. TBBPA and TCBPA induce lipid accumulation

3.2.1. Histopathology detection of liver changes

Oil Red O staining, which has the capacity to color lipid droplets, was used to identify the lipid droplets in *P. nigromaculatus* liver. Fig. 2C-L depicts the amounts of lipid buildup in the liver after treatment with TBBPA and TCBPA. There were very few lipid droplets in the control group (Fig. 2A), and DMSO treatment resulted in only few lipid droplets

Table 3
Real-time PCR primers.

Gene	GenBank Accession	Product Size (bp)	Oligonucleotide	Sequence real time PCR
GAPDH	FJ617544.1	245	Forward primer	GTCATCCCTGCTCTGAACGGAAAA
			Reverse primer	GCCTTCACTACGGCTTTGATGTCT
FAS	XM_012967541.1	84	Forward primer	GGAGAAGCCTTTAGCCGAGACC
			Reverse primer	GATGCGATTGGCAAACATAGCAC
ACC	NM_001137614.1	103	Forward primer	GAAAGAGCAATCCGTTTCGTGG
			Reverse primer	GTCCTCCTGGGACTGGCACAT
GPAT	NM_001079096.1	141	Forward primer	GACGTCCGTAAGAGCATGTTTTG
			Reverse primer	CTTCACTTTGTTGGTGGATTTGG
SREBP2	NM_001092085.1	102	Forward primer	GACGGTTACCCCTCACGTCCA
			Reverse primer	GGGCTGCCATCTGCCTTCAC
HMG-CoA	M29258.1	113	Forward primer	CTGGGAGGTCATCGTTGGGACT
			Reverse primer	CTTCAAACTTGGGGCAAGCATAA
PPARγ	M84163.1	106	Forward primer	GCCTCTGGGTTCCACTATGGC
			Reverse primer	GGCAATTCAGGTCGCACCTTTCA
RPL13A	From transcriptome	114	Forward primer	CAGAGCACCTAGCCGCATCTT
			Reverse primer	GGAGGTGGGATACCGTCAAAGA
Atg5	From transcriptome	77	Forward primer	CTGGGGAATACTCCATGAGCTTT
			Reverse primer	GTTGTGGATGGGTTTGCAGAAT
Atg7	From transcriptome	141	Forward primer	GCAGCCAAGTTTGTATCCAGGTAT
			Reverse primer	GCTGCTCTGGGTTTTGACACCT
P62	From transcriptome	79	Forward primer	GGTTACCCTGGCAGAGGCTTT
			Reverse primer	CAGGTGGAGTCTGACATTGTTCTG
Beclin1	From transcriptome	112	Forward primer	CTCCAGGCACCGTTTGTAGTTCT
			Reverse primer	GGATGTGGATCACCCTCTGTGT

All sequences are shown as 5′ → 3′. Annotated from the transcriptome (Liu et al., 2022).

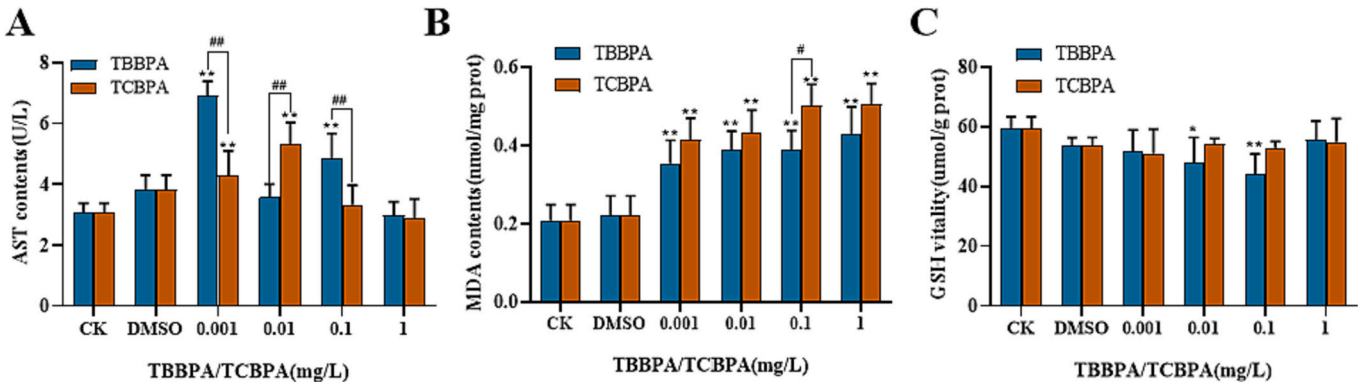

Fig. 1. the levels of transaminase in serum and MDA (malondialdehyde) contents and GSH (Glutathione) levels in the liver exposed TBBPA and TCBPA for 14 days. (A) Activities of AST (Glutamic oxalacetic transaminase), (B) MDA in the liver homogenates, (C) GSH in the liver homogenates. Bars represent the mean ± SEM. One-way analysis of variance was used to analyze the differences between the experimental data of the control group and the treatment group. Asterisk signs indicates that the experimental group is compared with the blank control group, well signs indicates that the TBBPA treatment group is compared with the TCBPA group at the same concentration (*$P < 0.05$, **$P < 0.01$, $^{\#}P < 0.05$, $^{\#\#}P < 0.01$).

(Fig. 2D). With the TBBPA (Fig. 2E-H) and TCBPA (Fig. 2I-L) treatments, lipid droplets accumulated in a dose-dependent manner. With higher dose treatment, the droplets increased in number and had larger volumes and deeper color. Liver from the 0.001 mg/L TBBPA group showed granulated lipid accumulation in hepatocytes (Fig. 2E). In Fig. 2H, there were more noticeable lipid droplets. They aggregated into larger droplets with exposure to 1 mg/L TBBPA (Fig. 2E) and 1 mg/L TCBPA (Fig. 2L). Similar levels of lipid accumulation were observed in groups treated with TCBPA and TBBPA.

3.2.2. *Effects of TBBPA and TCBPA on expression levels of TG and T-CHO genes*

To investigate how TBBPA and TCBPA affected formation of hepatic lipids, we determined the contents of T-CHO and TG. Only the 1 mg/L TCBPA group had a substantially raised T-CHO level (Fig. 2K, $P < 0.01$). The T-CHO contents were lower for TBBPA than TCBPA groups. The most pronounced differences between TBBPA and TCBPA were for those receiving 0.01 and 1 mg/L doses. Notably, the disparity between the 1 mg/L treatment groups was very substantial ($P < 0.01$), and the high concentration treatments contributed to T-CHO accumulation. The 1 mg/L TBBPA and TCBPA groups had very significant increases in TG levels (Fig. 2L). The TBBPA groups had lower TG levels than TCBPA, with extremely significant differences only between 1 mg/L treatment groups. High doses of TCBPA increased T-CHO contents, while high doses of TBBPA and TCBPA significantly increased TG contents.

3.2.3. *Effect of TBBPA and TCBPA on TG and T-CHO synthesis*

The proportional expression of *PPARγ* in the liver after 14 days of treatments with various amounts of TBBPA and TCBPA is shown in Fig. 3A. At 0.001, 0.01, 0.1, and 1 mg/L, the *PPARγ* expressions in the treatment groups were significantly higher than in control ($P < 0.05$). The *PPARγ* expression levels increased in a dose-dependent manner. The highest dose treatment group had the maximum levels of expression. Expression of *FAS* mRNA was significantly higher in the 0.01, 0.1, and 1 mg/L TBBPA and TCBPA groups (Fig. 3B, $P < 0.01$), and in the 0.001 mg/L TBBPA group ($P < 0.05$). However, there was no discernible distinction between the TBBPA and TCBPA treatments. Fig. 3C displays the proportional *ACC* mRNA levels in livers of the groups treated with

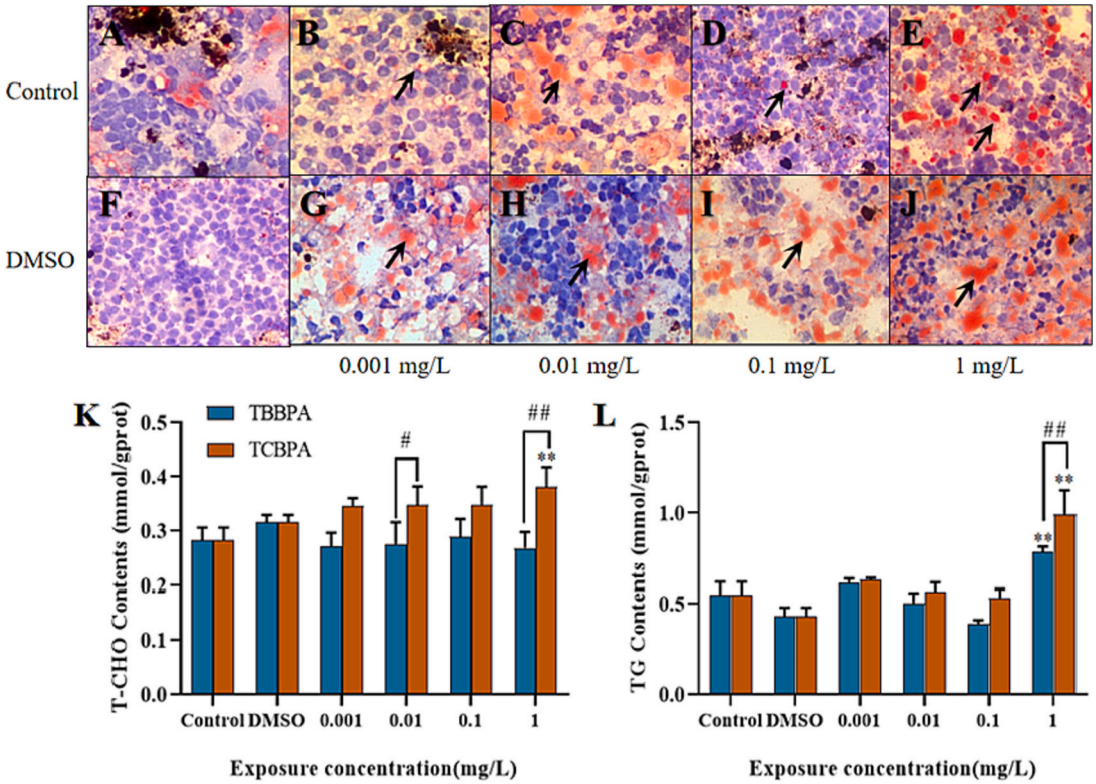

Fig. 2. Lipid droplets, T-CHO (total cholesterol) and TG (triglyceride) contents in the liver exposed to TBBPA and TCBPA for 14 days. (C) Control group; (D) DMSO group; (*E*-H) and (I-L) indicate TBBPA group and TCBPA group, respectively. Black arrows indicate the location of fat droplets. (A) T-CHO Contents in the liver; (B) TG Contents in the liver. One-way analysis of variance was used to analyze the differences between the experimental data of the control group and the treatment group. Asterisk signs indicate that the experimental group is compared with the blank control group, well signs indicate that the TBBPA treatment group is compared with the TCBPA group at the same concentration ($^{*}P < 0.05$, $^{**}P < 0.01$, $^{\#}P < 0.05$, $^{\#\#}P < 0.01$).

0.001, 0.01, 0.1, and 1 mg/L TBBPA and TCBPA. Compared to the control, the 0.01, 0.1, and 1 mg/L TBBPA and TCBPA groups had a significantly higher increase ($P < 0.01$). However, the results were comparable across the two treatment groups. Compared to the control, expression of *GPAT* increased significantly in both TBPPA and TCBPA treatments at dosages of 0.01, 0.1, and 1 mg/L (Fig. 3D, $P < 0.01$). In addition, the level was higher for 0.001 mg/L TCBPA compared to the control ($P < 0.05$). Furthermore, the 1 mg/L TBBPA group had significantly lower *GPAT* mRNA levels than the comparable TCBPA group ($P < 0.01$).

All treatment groups had significantly higher *SREBP2* mRNA relative expressions in the liver compared to the control ($P < 0.01$) (Fig. 3E). Furthermore, between the TBBPA and TCBPA treatments, in 0.01, 0.1, and 1 mg/L groups, there were significant increases in expression of hepatic *SREBP2* mRNA. The *HMG-CoA* mRNA expressions in liver were significantly higher in the 0.01, 0.1, and 1 mg/L TBBPA and TCBPA groups compared to control (Fig. 3F, $P < 0.01$). These revealed substantial rises in the 0.01, 0.1, and 1 mg/L treatment groups compared to the control.

3.2.4. PPARγ-binding potential of TBBPA and TCBPA

We conducted molecular docking to analyze the binding potential of TBBPA and TCBPA with PPARγ amino acid residues. The results indicated that TCBPA formed a hydrogen bond with the hydroxyl group of PPARγ via residues ALA-346 and ASP-347 on the side chain. Meanwhile, the oxygen atom on the TBBPA ligand formed hydrogen bonds with the hydrogen atom on the PPAR receptor protein's GLN-290 residues. The binding energy between TBBPA and PPARγ was −6.4 kcal/mol, and between TCBPA and PPARγ was −7.9 kcal/mol (Table 4). These results showed that TBBPA and TCBPA had binding potential with PPARγ protein receptors in *P. nigromaculatus* (Fig. 3G).

3.3. Expression of autophagy-related genes

The levels of autophagy-related transcripts showed that TBBPA and TCBPA increased *Atg5/7* and *Beclin1* mRNA expression (Fig. 4A–C), while down-regulating the level of *P62* (Fig. 4D). Our findings indicated that TBBPA and TCBPA caused liver oxidative injury in frogs and stimulated cell autophagy. Genes involved in autophagy underwent dose-dependent changes at the transcript level. Compared to controls, the TBBPA and TCBPA groups had noticeably higher *Atg5* expression levels at 0.1 and 1 mg/L (Fig. 4B), and the 0.01, 0.1, and 1 mg/L TBBPA and TCBPA groups had substantially raised *Atg7* transcript levels (Fig. 4A). In all treatment groups, there was a significant rise in expression of *Beclin1* mRNA, but this was more pronounced in the 0.1 and 1 mg/L TCBPA groups than in the 0.1 and 1 mg/L TBBPA group (Fig. 4C). However, expression of *P62* dropped in a dose-dependent fashion, with a noticeably greater decline for the 0.001 mg/L TCBPA group than the 0.01, 0.1, and 1 mg/L TBBPA and TCBPA groups (Fig. 4D). Overall, the results showed that TCBPA had a stronger effect on frog liver than TBBPA.

4. Discussion

Study revealed that TBBPA and TCBPA could lead to lipid accumulation in zebrafish liver, and finally might contribute to development of obesity (Riu et al., 2014). However, the impacts of BFR on liver toxicity and their potential molecular pathwaysof frog remain poorly understood to date. The results obtained in present study showed that exposure to two commonly used BFR (TBBPA and TCBPA) exerted liver toxicity on the black-spotted frog *P. nigromaculatus*, whcih might cause by alteration in special cellular and molecular processes.

The activity of AST is one of the most common indicators for

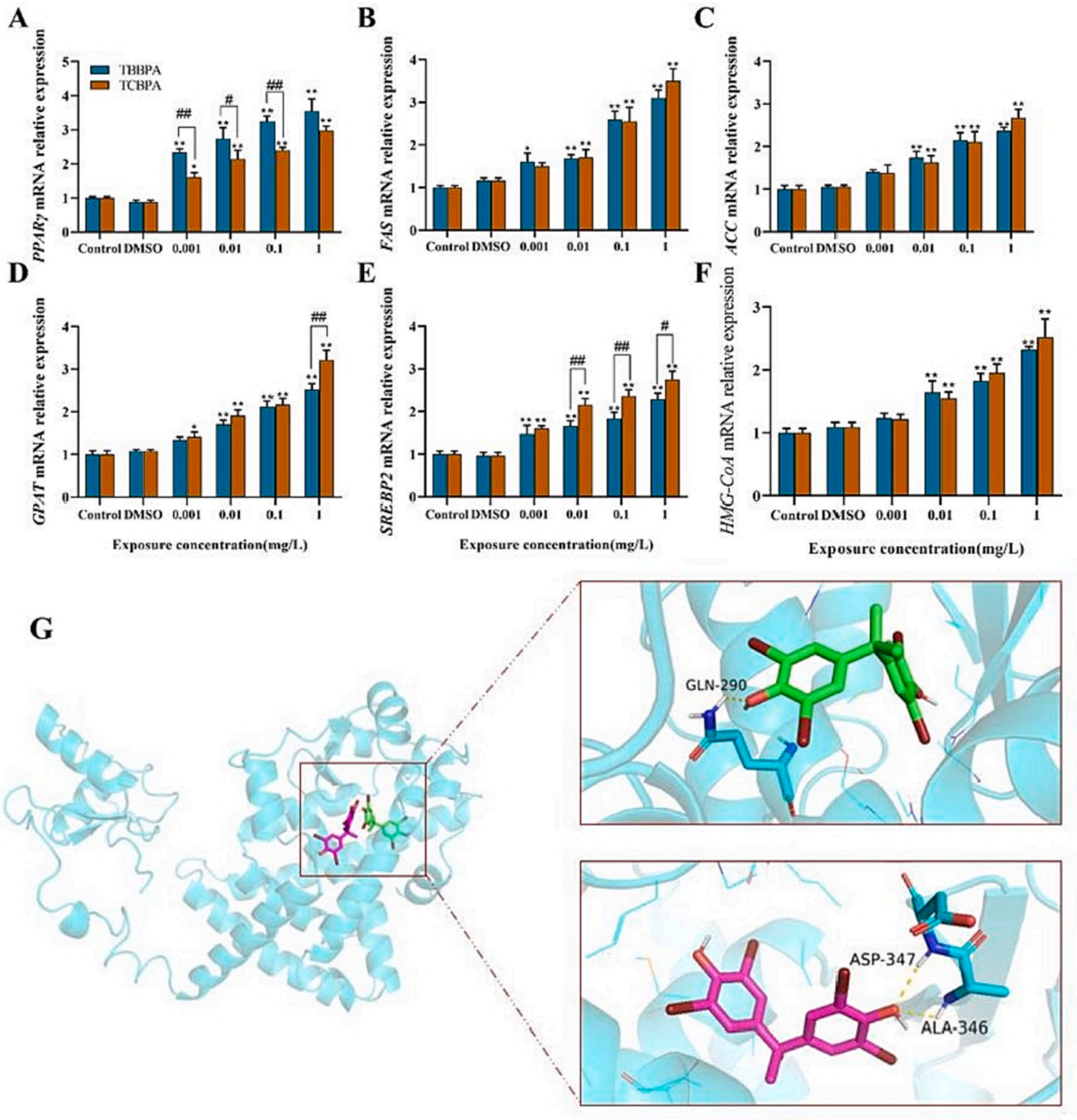

Fig. 3. Relative mRNA expression of *PPARγ* (*Peroxisome Proliferator-activated receptor gamma*), *SREBP2* (*sterol regulatory element-binding protein 2*) and *HMG-CoA* (*3-hydroxy-3-methylglutaryl*) mRNA in the liver of *P. nigromaculatus* after 14 days of exposure to TBBPA and TCBPA, along with molecular docking results. (A-F) Relative expression level of *PPARγ (peroxisome proliferator-activated receptor gamma)*, *FAS (fatty acid synthase)*, *ACC (acetylCoA carboxylase)*, *GPAT (acetylCoA carboxylase)*, *SREBP2 (sterol regulatory element-binding protein 2)* and *HMG-CoA (3-hydroxy-3-methylglutaryl CoA)* mRNA in the liver, separately. One-way analysis of variance was used to analyze the differences between the experimental data of the control group and the treatment group. Bars represent mean ± SEM. Asterisk signs indicate that the experimental group is compared with the blank control group, well signs indicate that the TBBPA treatment group is compared with the TCBPA group at the same concentration ($^{*}P < 0.05$, $^{**}P < 0.01$, $^{\#}P < 0.05$, $^{\#\#}P < 0.01$). (G) Results of molecular docking between BPA and PPARγ, the TBBPA was represented by green sticks, the TCBPA by magenta sticks, and the PPAR protein by a cyan caricature. The residues in the binding compartments and their environs are represented by cyan sticks. The hydrogen bond is represented by the yellow dashed lines.

Table 4
The lowest binding energies for TCBPA and TBBPA to the PPAR active site.

Proteins	Pollutant	Binding energy (kcal/mol)	Binding sites
PPARγ	TBBPA	−6.4	GLN-290
	TCBPA	−7.9	ALA-346, ASP-347

evaluating liver function (Jakubczyk et al., 2020). In addition, the level of GSH and MDA in liver also play an important role in regulating liver homeostasis (Hu et al., 2019). AST activity in the liver of freshwater crucian carp increased considerably after 4, 8, and 16 days of TBBPA exposure, causing abnormal liver function (Yang et al., 2013). Furthermore, MDA expression level in human breast cancer cells

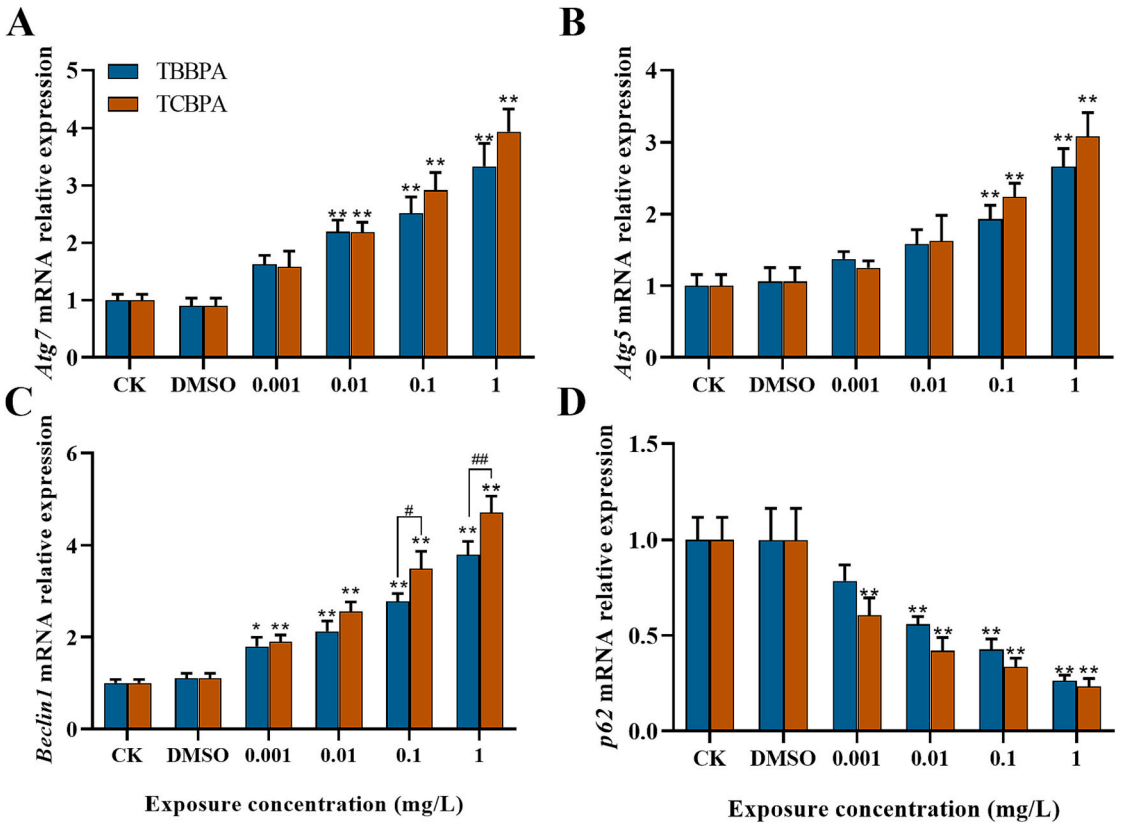

Fig. 4. Relative autophagy-related genes in the liver in the liver exposed to TBBPA and TCBPA for 14 days. (A-C) Relative expression level of *Atg7*, *Atg5*, *Beclin1*and *p62* mRNA in the liver in proper order. One-way analysis of variance was used to analyze the differences between the experimental data of the control group and the treatment group. Bars represent mean ± SEM. Asterisk signs indicates that the experimental group is compared with the blank control group, well signs indicates that the TBBPA treatment group is compared with the TCBPA group at the same concentration ((*$P < 0.05$, **$P < 0.01$, $^{\#}P < 0.05$, $^{\#\#}P < 0.01$).

increased while the GSH level decreased after exposure to TBBPA and TCBPA for a certain period, leading to a significant increase in lipid peroxidation (Zhao et al., 2019). Consistent with previous findings, results in present study found that TBBPA and TCBPA significantly increased the activity of AST liver enzymes of serum (Fig. 1A), raise MDA accumulation (Fig. 1B) and decreased GSH content in liver of frog (Fig. 1C). The above results indicated that TBBPA and TCBPA induced lipid peroxidation of frog liver, which might be a reason for abnormal liver function.

It's commonly known that oxidative stress could regulate lipid homeostasis (Chen et al., 2022). Oil Red O staining showed that liver lipid accumulation of frog was dose depend along with TBBPA and TCBPA after 14 days exposure (Fig. 2A–J). In addition, TBBPA and TCBPA could significantly increase T-CHO and TG levels of frog liver in high concentrations (Fig. 2K and L). Based on related studies, the quantity of lipid accumulation in juvenile zebrafish exposed to TBBPA and TCBPA was significantly greater than the control group. Other study revealed that TBBPA and TCBPA enhanced lipid accumulation in HepG2 cells, and TCBPA had more impact (Liu et al., 2020). Similarly, the lipid droplets of TCBPA group were larger than TBBPA in present study. In summary, our research suggested that the *P. nigromaculatus* liver was impaired when exposed to TBBPA and TCBPA, which caused lipid deposition and altered gene expression levels.

As a member of the nuclear hormone receptor superfamily, PPARγ has the ability to regulate lipid production (Yang et al., 2018). Studies have shown that TBBPA and TCBPA can modulate and stimulate PPARγ (Riu et al., 2011; Fang et al., 2015; Cheng et al., 2022). In our experiments, TBBPA and TCBPA were markedly interrupting *PPARγ* expression (Fig. 3A), which might promote lipid accumulation in frog liver. Molecular docking simulation is a reliable method for determining probable interactions between substances and proteins (Ding et al., 2017). The stable hydrogen bond binding sites between the receptor and the ligand can be formed with the help of binding energy, indicating docking activity between the ligand and the receptor. Hydrogen bonds play an important role in connecting protein receptor residues with molecular ligands (Chen et al., 2019). In this study, TCBPA ligands bound to PPARγ residues ALA-346 and ASP-347 via hydrogen bonds, while TBBPA formed hydrogen bonds with PPARγ protein receptor residues GLN-290 through hydrogen atoms. Furthermore, the affinities of TBBPA and TCBPA were − 6.4 and − 7.9 kcal/mol respectively. These results suggested that TCBPA could embed into the binding domain of the receptor protein easier, and had stronger docking activity than TBBPA. Molecular ligands and protein receptors combine to create a complex which might threat to organisms. For example, bis(2-ethylhexyl)-2,3,4,5-tetrabromophthalate could interact with PPARγ residues HIS199, PRO176, and LIE153, the binding of residues ultimately affected the lipid metabolism and disrupted energy homeostasis of juvenile zebrafish (Guo et al., 2020). In our research, molecular docking showed that both TBBPA and TCBPA were capable of binding to PPARγ, which might be another factor affecting lipid accumulation in frog liver.

PPARγ responsive genes include those related to adipogenesis, such as ACC and FAS, and GPAT responsible for TG synthesis (Li et al., 2022b). In our study, expression of *FAS*, *ACC* and *GPAT* were significantly increased after 14 days of exposure to TBBPA and TCBPA (Fig. 3B-D). Hence, the absence of TBBPA and TCBPA might interrupt fat synthesis via alter regulating *FAS*, *ACC* and *GPAT* expression. Furthermore, SREBPs, a subgroup of transcription factors, include the fundamental helix-loop-helix-leucine zipper (Miyata et al., 2022). The SREBPs (SREBP1 and SREBP2) and HMG-CoA play an important role in maintain

liposome balance and transcription (Cheng et al., 2022; Kowalczyk et al., 2023; Li et al., 2022a). With 14 days of treatment, the relative transcription levels of *SREBP2* and *HMG-CoA* were increased (Fig. 3E, F). Therefore, TBBPA and TCBPA might initiate mechanism to promote TG accumulation in frog liver.

Autophagy can be activated and inhibited by rapamycin (Rapa) and chloroquine (CQ), respectively. In addition, reactive stress was known to activate autophagy, which could have beneficial or harmful effects on cell survival. Previous study showed that *Atg5*, *Atg7, Beclin-1* and *p62* involved in initiate of autophagy (Kuma and Mizushima, 2010; Hasan et al., 2020). Our findings indicated that TBBPA and TCBPA significantly upregulated *Atg5/7* and *Beclin1* mRNA expression levels while substantially downregulated *p62* expression levels (Fig. 4A–D), suggesting that both TBBPA and TCBPA induced autophagy in *P. nigromaculatus* liver.

5. Conclusion

This study demonstrated that exposure to high doses of TBBPA and TCBPA induced cellular autophagy, caused oxidative stress and lipid accumulation in liver of *P. nigromaculatus*. In addition, TBBPA and TCBPA influenced the expression of lipid metabolism related genes. However, the precise mechanisms by which these impacts occur require further investigation. Furthermore, there is a lack of toxicity research based on the TBBPA and TCBPA molecular structures related to biotoxicity, and additional research is necessary to identify the underlying biochemical mechanism. This research project also aimed to elucidate the biochemical mechanism of the lipid biosynthesis pathway. The potential implications of these findings for environmental and public health are significant, as TBBPA and TCBPA are commonly used in a variety of consumer products and have been detected in the environment. These compounds may pose a risk to aquatic organisms and could potentially have negative effects on human health through contaminated food or water sources. Therefore, it is crucial to continue investigating the toxic effects of these chemicals and to develop measures to minimize their release into the environment.

Supplementary data to this article can be found online at https://doi.org/10.1016/j.scitotenv.2023.166421.

Author contributions statement

Yu Han: Experimental design, Investigation, Data curation and analysis, Writing – review, editing & revision.

Hongmei Yang: Conceptualization, Methodology, Resources, Formal analysis, Investigation, Data curation, Writing – original draft, Writing –review & editing.

Zhiqun Liu: Conceptualization, Methodology, Resources, Visualization, Data curation, Writing – review & editing.

Chao Hu: Writing – original draft, Writing – review & editing.

Imane Lamine: Conceptualization, Methodology, Resources, Visualization, Funding acquisition, Writing – review & editing.

Zhiquan Liu: Conceptualization, Methodology, Writing – review & editing.

Panpan Gao: Conceptualization, Methodology, Writing – review & editing.

Yanming Sui: Conceptualization, Methodology, Resources, Writing - re-view & editing.

Pei Zhen: Conceptualization, Methodology, Resources, Writing - review & editing. Hangjun Zhang: Conceptualization, Methodology, Data curation.

Xiuying Jia: Conceptualization, Methodology, *Re*-sources, Visualization, Supervision, Writing – review & editing, Project administration, Funding acquisition.

Declaration of competing interest

This manuscript has not been published or presented elsewhere in part or in entirety and is not under consideration by another journal. We have read and understood the journal's policies, and we believe that neither the manuscript nor the study violates any of these. There are no conflicts of interest to declare.

Data availability

Data will be made available on request.

Acknowledgments

This work was financially supported by the Natural Science Foundation of Zhejiang Province of China (LQ22C030003), the National Natural Science Foundation of China (42207323), the special fund of State Environmental Protection Key Laboratory of Environmental Health Impact Assessment of Emerging Contaminants (SEPKL-EHIAEC-202201), and the Scientific Research Foundation for Scholars of Hangzhou Normal University (2021QDL063).

References

Baranska, A., Wozniak, A., Mokra, K., Michalowicz, J., 2022. Genotoxic mechanism of action of TBBPA, TBBPS and selected bromophenols in human peripheral blood mononuclear cells. Front. Immunol. 13, 869741.

Bjermo, H., Aune, M., Cantillana, T., Glynn, A., Lind, P.M., Ridefelt, P., Darnerud, P.O., 2017. Serum levels of brominated flame retardants (BFRs: PBDE, HBCD) and influence of dietary factors in a population-based study on Swedish adults. Chemosphere 167, 485–491.

Chen, G.H., Song, C.C., Zhao, T., Hogstrand, C., Wei, X.L., Lv, W.H., Song, Y.F., Luo, Z., 2022. Mitochondria-dependent oxidative stress mediates ZnO nanoparticle (ZnO NP)-induced mitophagy and lipotoxicity in freshwater teleost fish. Environ. Sci. Technol. 56, 2407–2420.

Chen, Z., Yao, X., Dong, F., Duan, H., Shao, X., Chen, X., Yang, T., Wang, G., Zheng, Y., 2019. Ecological toxicity reduction of dinotefuran to honeybee: new perspective from an enantiomeric level. Environ. Int. 130, 104854.

Cheng, C., Geng, F., Li, Z., Zhong, Y., Wang, H., Cheng, X., Zhao, Y., Mo, X., Horbinski, C., Duan, W., Chakravarti, A., Cheng, X., Guo, D., 2022. Ammonia stimulates SCAP/Insig dissociation and SREBP-1 activation to promote lipogenesis and tumour growth. Nat Metab 4, 575–588.

Choi, C.G., Lee, D.J., Chung, N., Joo, Y.H., 2022. Anti-obesity effects of isoacteoside on 3T3-L1 adipocytes. Applied. Biol. Chem. 65.

Ding, K., Kong, X., Wang, J., Lu, L., Zhou, W., Zhan, T., Zhang, C., Zhuang, S., 2017. Side chains of parabens modulate antiandrogenic activity: in vitro and molecular docking studies. Environ. Sci. Technol. 51, 6452–6460.

Fang, M., Webster, T.F., Stapleton, H.M., 2015. Activation of Human Peroxisome Proliferator-Activated Nuclear Receptors (PPARgamma1) by Semi-Volatile Compounds (SVOCs) and Chemical Mixtures in Indoor Dust. Environ. Sci. Technol. 49, 10057–10064.

Garoche, C., Boulahtouf, A., Grimaldi, M., Chiavarina, B., Toporova, L., den Broeder, M. J., Legler, J., Bourguet, W., Balaguer, P., 2021. Interspecies differences in activation of peroxisome proliferator-aactivated receptor gamma by pharmaceutical and environmental chemicals. Environ. Sci. Technol. 55, 16489–16501.

Gong, D., Sun, K., Yin, K., Wang, X., 2023. Selenium mitigates the inhibitory effect of TBBPA on NETs release by regulating ROS/MAPK pathways-induced carp neutrophil apoptosis and necroptosis. Fish Shellfish Immunol 132, 108501.

Guo, W., Han, J., Wu, S., Shi, X., Wang, Q., Zhou, B., 2020. Bis(2-ethylhexyl)-2,3,4,5-tetrabromophthalate affects lipid metabolism in zebrafish larvae via DNA methylation modification. Environ. Sci. Technol. 54, 355–363.

Hasan, A., Haque, E., Hameed, R., Maier, P.N., Irfan, S., Kamil, M., Nazir, A., Mir, S.S., 2020. Hsp90 inhibitor gedunin causes apoptosis in A549 lung cancer cells by disrupting Hsp90: Beclin-1: Bcl-2 interaction and downregulating autophagy. Life Sci. 256, 118000.

He, M.J., Luo, X.J., Yu, L.H., Wu, J.P., Chen, S.J., Mai, B.X., 2013. Diasteroisomer and enantiomer-specific profiles of hexabromocyclododecane and tetrabromobisphenol a in an aquatic environment in a highly industrialized area, South China: vertical profile, phase partition, and bioaccumulation. Environ. Pollut. 179, 105–110.

Hu, C., Zhao, L., Tao, J., Li, L., 2019. Protective role of melatonin in early-stage and end-stage liver cirrhosis. J. Cell. Mol. Med. 23, 7151–7162.

Huang, M., Li, J., Xiao, Z., Shi, Z., 2020. Tetrabromobisphenol a and hexabromocyclododecane isomers in breast milk from the general population in Beijing, China: contamination levels, temporal trends, nursing infant's daily intake, and risk assessment. Chemosphere 244, 125524.

Huo, R., Zhang, M., Zhang, Y., Bai, X., Zhang, Y., Guo, X., 2022. Effects of oat complex high-fiber formula powder on the composition of intestinal microbiota and enzyme activities in mice induced by a high-fat diet. Front Nutr 9, 871556.

IUCN, 2023. The IUCN Red List of Threatened Species, Version 2021-3. https://www.iucnredlist.org..
Jakubczyk, K., Skonieczna-Zydecka, K., Kaldunska, J., Stachowska, E., Gutowska, I., Janda, K., 2020. Effects of resveratrol supplementation in patients with non-alcoholic fatty liver disease-a meta-analysis. Nutrients 12.
Jarosiewicz, M., Duchnowicz, P., Wluka, A., Bukowska, B., 2017. Evaluation of the effect of brominated flame retardants on hemoglobin oxidation and hemolysis in human erythrocytes. Food Chem. Toxicol. 109, 264–271.
Jia, X., Yan, R., Lin, H., Liu, Z., Shen, L., Yang, H., Wu, H., Shan, X., Zhang, H., 2022. TBBPA and its alternative TCBPA induced ROS-dependent mitochondria-mediated apoptosis in the liver of *Rana nigromaculata*. Environ. Pollut. 297, 118791.
Kim, U.J., Lee, I.S., Oh, J.E., 2016. Occurrence, removal and release characteristics of dissolved brominated flame retardants and their potential metabolites in various kinds of wastewater. Environ. Pollut. 218, 551–557.
Kowalczyk, M., Piwowarski, J.P., Wardaszka, A., Srednicka, P., Wojcicki, M., Juszczuk-Kubiak, E., 2023. Application of in vitro models for studying the mechanisms underlying the obesogenic action of eendocrine-disrupting chemicals (EDCs) as food contaminants-a review. Int. J. Mol. Sci. 24.
Kuma, A., Mizushima, N., 2010. Physiological role of autophagy as an intracellular recycling system: with an emphasis on nutrient metabolism. Semin. Cell Dev. Biol. 21, 683–690.
Law, R.J., Allchin, C.R., de Boer, J., Covaci, A., Herzke, D., Lepom, P., Morris, S., Tronczynski, J., de Wit, C.A., 2006. Levels and trends of brominated flame retardants in the European environment. Chemosphere 64, 187–208.
Lee, E., Bang, J., Lee, J.Y., Jun, W., Lee, Y.H., 2022. Anti-obesity effect of porcine collagen peptide in 3T3-L1 adipocytes and high-fat diet-fed mice by regulating adipogenesis. J. Med. Food 25, 732–740.
Lent, E.M., Babbitt, K.J., Pinkney, A.E., 2021. Effects of environmental contaminants at great bay national wildlife refuge on anuran development, gonadal histology, and reproductive steroidogenesis: a comparison of in situ and laboratory exposures. Arch. Environ. Contam. Toxicol. 80, 663–679.
Li, J., Shen, H., Owens, G.K., Guo, L.W., 2022a. SREBP1 regulates Lgals3 activation in response to cholesterol loading. Mol Ther Nucleic Acids 28, 892–909.
Li, S., Lu, C.W., Diem, E.C., Li, W., Guderian, M., Lindenberg, M., Kruse, F., Buettner, M., Floess, S., Winny, M.R., Geffers, R., Richnow, H.H., Abraham, W.R., Grassl, G.A., Lochner, M., 2022b. Acetyl-CoA-carboxylase 1-mediated de novo fatty acid synthesis sustains Lgr5(+) intestinal stem cell function. Nat. Commun. 13, 3998.
Li, A., Zhuang, T., Shi, W., Liang, Y., Liao, C., Song, M., Jiang, G., 2020. Serum concentration of bisphenol analogues in pregnant women in China. Sci. Total Environ. 707, 136100.
Liu, Q., Shao, W., Weng, Z., Zhang, X., Ding, G., Xu, C., Xu, J., Jiang, Z., Gu, A., 2020. In vitro evaluation of the hepatic lipid accumulation of bisphenol analogs: a high-content screening assay. Toxicol. in Vitro 68, 104959.
Lin, H., Liu, Z., Yang, H., Lu, L., Chen, R., Zhang, X., Zhong, Y., Zhang, H., 2022a. Per- and polyfluoroalkyl substances (PFASs) impair lipid metabolism in *Rana nigromaculata*: a field investigation and laboratory study. Environ. Sci. Technol. 56, 13222–13232.
Lin, H., Wu, H., Liu, F., Yang, H., Shen, L., Chen, J., Zhang, X., Zhong, Y., Zhang, H., 2022b. Assessing the hepatotoxicity of PFOA, PFOS, and 6:2 Cl-PFESA in black-spotted frogs (Rana nigromaculata) and elucidating potential association with gut microbiota. Environ. Pollut. 312, 120029.
Liu, W., Pan, Y., Yang, L., Xie, Y., Chen, X., Chang, J., Hao, W., Zhu, L., Wan, B., 2023. Developmental toxicity of TCBPA on the nervous and cardiovascular systems of zebrafish (*Danio rerio*): a combination of transcriptomic and metabolomics. J. Environ. Sci. (China) 127, 197–209.
Luo, J., Yang, H., Song, B.L., 2020. Mechanisms and regulation of cholesterol homeostasis. Nat Rev Mol Cell Biol 21, 225–245.
Ma, M., Crump, D., Farmahin, R., Kennedy, S.W., 2015. Comparing the effects of tetrabromobisphenol-a, bisphenol a, and their potential replacement alternatives, TBBPA-bis (2,3-dibromopropyl ether) and bisphenol S, on cell viability and messenger ribonucleic acid expression in chicken embryonic hepatocytes. Environ. Toxicol. Chem. 34, 391–401.
Miyata, S., Kodaka, M., Kikuchi, A., Matsunaga, Y., Shoji, K., Kuan, Y.C., Iwase, M., Takeda, K., Katsuta, R., Ishigami, K., Matsumoto, Y., Suzuki, T., Yamamoto, Y., Sato, R., Inoue, J., 2022. Sulforaphane suppresses the activity of sterol regulatory element-binding proteins (SREBPs) by promoting SREBP precursor degradation. Sci. Rep. 12, 8715.
Moore, M.N., Kohler, A., Lowe, D., Viarengo, A., 2008. Lysosomes and autophagy in aquatic animals. Methods Enzymol. 451, 581–620.
Nguyen, T.B., Louie, S.M., Daniele, J.R., Tran, Q., Dillin, A., Zoncu, R., Nomura, D.K., Olzmann, J.A., 2017. DGAT1-dependent lipid droplet biogenesis protects mitochondrial function during starvation-induced autophagy. Dev. Cell 42 (9–21), e25.
Pan, Y.X., Luo, Z., Zhuo, M.Q., Wei, C.C., Chen, G.H., Song, Y.F., 2018. Oxidative stress and mitochondrial dysfunction mediated cd-induced hepatic lipid accumulation in zebrafish *Danio rerio*. Aquat. Toxicol. 199, 12–20.
Riu, A., Grimaldi, M., le Maire, A., Bey, G., Phillips, K., Boulahtouf, A., Perdu, E., Zalko, D., Bourguet, W., Balaguer, P., 2011. Peroxisome proliferator-activated receptor gamma is a target for halogenated analogs of bisphenol A. Environ. Health Perspect. 119, 1227–1232.
Riu, A., McCollum, C.W., Pinto, C.L., Grimaldi, M., Hillenweck, A., Perdu, E., Zalko, D., Bernard, L., Laudet, V., Balaguer, P., Bondesson, M., Gustafsson, J.A., 2014. Halogenated bisphenol-a analogs act as obesogens in zebrafish larvae (*Danio rerio*). Toxicol. Sci. 139, 48–58.
Shibata, M., Yoshimura, K., Furuya, N., Koike, M., Ueno, T., Komatsu, M., Arai, H., Tanaka, K., Kominami, E., Uchiyama, Y., 2009. The MAP1-LC3 conjugation system is involved in lipid droplet formation. Biochem. Biophys. Res. Commun. 382, 419–423.
Shibata, M., Yoshimura, K., Tamura, H., Ueno, T., Nishimura, T., Inoue, T., Sasaki, M., Koike, M., Arai, H., Kominami, E., Uchiyama, Y., 2010. LC3, a microtubule-associated protein1A/B light chain3, is involved in cytoplasmic lipid droplet formation. Biochem. Biophys. Res. Commun. 393, 274–279.
Siviter, H., Bailes, E.J., Martin, C.D., Oliver, T.R., Koricheva, J., Leadbeater, E., Brown, M.J.F., 2021. Agrochemicals interact synergistically to increase bee mortality. Nature 596, 389–392.
Song, M., Liang, D., Liang, Y., Chen, M., Wang, F., Wang, H., Jiang, G., 2014a. Assessing developmental toxicity and estrogenic activity of halogenated bisphenol a on zebrafish (*Danio rerio*). Chemosphere 112, 275–281.
Song, S., Song, M., Zeng, L., Wang, T., Liu, R., Ruan, T., Jiang, G., 2014b. Occurrence and profiles of bisphenol analogues in municipal sewage sludge in China. Environ. Pollut. 186, 14–19.
Su, L., Zhou, L., Chen, F.J., Wang, H., Qian, H., Sheng, Y., Zhu, Y., Yu, H., Gong, X., Cai, L., Yang, X., Xu, L., Zhao, T.J., Li, J.Z., Chen, X.W., Li, P., 2019. Cideb controls sterol-regulated ER export of SREBP/SCAP by promoting cargo loading at ER exit sites. EMBO J. 38.
Su, Y., Quan, C., Li, X., Shi, Y., Duan, P., Yang, K., 2018. Mutual promotion of apoptosis and autophagy in prepubertal rat testes induced by joint exposure of bisphenol a and nonylphenol. Environ. Pollut. 243, 693–702.
Tang, J., Jia, X., Gao, N., Wu, Y., Liu, Z., Lu, X., Du, Q., He, J., Li, N., Chen, B., Jiang, J., Liu, W., Ding, Y., Zhu, W., Zhang, H., 2018. Role of the Nrf2-ARE pathway in perfluorooctanoic acid (PFOA)-induced hepatotoxicity in Rana nigromaculata. Environ. Pollut. 238, 1035–1043.
Yang, S., Wang, S., Liu, H., Yan, Z., 2012. Tetrabromobisphenol a: tissue distribution in fish, and seasonal variation in water and sediment of Lake Chaohu, China. Environ. Sci. Pollut. Res. Int. 19, 4090–4096.
Yang, S., Xu, F., Zheng, B., Wu, F., Wang, S., 2013. Multibiomarker responses upon exposure to tetrabromobisphenol a in the freshwater fish *Carassius auratus*. Aquat. Toxicol. 142-143, 248–256.
Yang, W., Yang, C., Luo, J., Wei, Y., Wang, W., Zhong, Y., 2018. Adiponectin promotes preadipocyte differentiation via the PPAR gamma pathway. Mol. Med. Rep. 17, 428–435.
Yao, L., Wang, Y., Shi, J., Liu, Y., Guo, H., Yang, X., Liu, Y., Ma, J., Li, D., Wang, Z., Li, Z., Luo, Q., Fu, J., Zhang, Q., Qu, G., Wang, Y., Jiang, G., 2021. Toxicity of Tetrabromobisphenol a and its derivative in the mouse liver following oral exposure at environmentally relevant levels. Environ. Sci. Technol. 55, 8191–8202.
Yu, Y., Hao, C., Xiang, M., Tian, J., Kuang, H., Li, Z., 2022. Potential obesogenic effects of TBBPA and its alternatives TBBPS and TCBPA revealed by metabolic perturbations in human hepatoma cells. Sci. Total Environ. 832, 154847.
Yu, Y., Yu, Z., Chen, H., Han, Y., Xiang, M., Chen, X., Ma, R., Wang, Z., 2019. Tetrabromobisphenol A: disposition, kinetics and toxicity in animals and humans. Environ. Pollut. 253, 909–917.
Yuan, S.Y., Li, H.T., Huang, H.W., Chang, B.V., 2010. Biodegradation of tetrachlorobisphenol-a in river sediment and the microbial community changes. J. Environ. Sci. Health B 45, 360–365.
Zhang, H., Liu, W., Chen, B., He, J., Chen, F., Shan, X., Du, Q., Li, N., Jia, X., Tang, J., 2018. Differences in reproductive toxicity of TBBPA and TCBPA exposure in male *Rana nigromaculata*. Environ. Pollut. 243, 394–403.
Zhang, H., He, J., Li, N., Gao, N., Du, Q., Chen, B., Chen, F., Shan, X., Ding, Y., Zhu, W., Wu, Y., Tang, J., Jia, X., 2019. Lipid accumulation responses in the liver of *Rana nigromaculata* induced by perfluorooctanoic acid (PFOA). Ecotoxicol. Environ. Saf. 167, 29–35.
Zhang, W., Sun, S., Du, X., Han, Y., Tang, Y., Zhou, W., Shi, W., Liu, G., 2022. Toxic impacts of microplastics and tetrabromobisphenol a on the motility of marine microalgae and potential mechanisms of action. Gondwana Res. 108, 158–170.
Zhao, C., Tang, Z., Chung, A.C.K., Wang, H., Cai, Z., 2019. Metabolic perturbation, proliferation and reactive oxygen species jointly contribute to cytotoxicity of human breast cancer cell induced by tetrabromo and tetrachloro bisphenol a. Ecotoxicol. Environ. Saf. 170, 495–501.
Zhao, X.J., Yu, H.W., Yang, Y.Z., Wu, W.Y., Chen, T.Y., Jia, K.K., Kang, L.L., Jiao, R.Q., Kong, L.D., 2018. Polydatin prevents fructose-induced liver inflammation and lipid deposition through increasing miR-200a to regulate Keap1/Nrf2 pathway. Redox Biol. 18, 124–137.